Sensitization of Tumor to [212]Pb-radioimmunotherapy by gemcitabine involves initial abrogation of G2 arrest and blocked DNA damage repair by interference with Rad51

Kwon Joong Yong, Ph.D., **Diane E. Milenic, M.S.**, **Kwamena E. Baidoo, Ph.D.**, and **Martin W. Brechbiel, Ph.D.**[*]
Radioimmune & Inorganic Chemistry Section, Radiation Oncology Branch, National Cancer Institute, National Institutes of Health, Bethesda MD

Abstract

Purpose—To elucidate the mechanism of the therapeutic efficacy of targeted α-particle radiation therapy using [212]Pb-TCMC-trastuzumab together with gemcitabine (Gem) for treatment of disseminated peritoneal cancers.

Methods and Materials—Mice bearing human colon cancer LS-174T i.p. xenografts were pre-treated with Gem, followed by [212]Pb-TCMC-trastuzumab and compared to controls.

Results—Treatment with [212]Pb-TCMC-trastuzumab increased the apoptotic rate in the S-phase arrested tumors induced by Gem at earlier time points (6 to 24 hours). [212]Pb-TCMC-trastuzumab after Gem pre-treatment abrogated G2/M arrest at the same time points, which may be associated with the inhibition of Chk1 phosphorylation and, in turn, cell cycle perturbation, resulting in apoptosis. [212]Pb-TCMC-trastuzumab treatment post-Gem pre-treatment caused depression of DNA synthesis, DNA double strand breaks, accumulation of unrepaired DNA, and down-regulation of Rad51 protein, indicating that DNA damage repair was blocked. In addition, modification in the chromatin structure of *p21* may be associated with transcriptionally repressed chromatin states, indicating the open structure was delayed at earlier time points.

Conclusion—These findings suggest that the cell killing efficacy of [212]Pb-TCMC-trastuzumab following Gem pre-treatment may be associated with abrogation of G2/M checkpoint, inhibition of DNA damage repair, and chromatin remodeling.

INTRODUCTION

Pancreatic and ovarian cancers remain two of the least curable cancers (1). The prognosis on these cancers continues to be poor and requires a high priority for the development of new therapeutic strategies and diagnostic modalities.

Gemcitabine (Gem; $2'$, $2'$-difluoro-$2'$-deoxycytidine), is a nucleoside analogue that inhibits DNA synthesis that has been found to have therapeutic efficacy as a single modality against a variety of tumors (2). Although Gem has also been used clinically as a radiation sensitizer, standard radiotherapy procedures do not easily or efficiently treat distant, undetected

Correspondence to: Martin W. Brechbiel, Ph.D. Radioimmune & Inorganic Chemistry Section, Radiation Oncology Branch, NCI, NIH, 10 Center Drive MSC-1002, Room 1B53, Bethesda, MD 20892-1088, Fax: (301) 402-1923 martinwb@mail.nih.gov.

Conflict of interest: none

metastatic or disseminated disease. Targeted radiation therapy with monoclonal antibodies (mAbs), which bind to tumor-associated antigens, may be efficacious in a coordinated strategy (3).

Lead-212, a promising α-particle emitting source has been successfully used in targeted RIT and pre-targeted RIT (3). Although synergistic effects of α-emitting radionuclides with chemotherapeutics on cancer cells have been reported (4, 5), the mechanisms of cell death induced by the targeted delivery of high LET radiation are poorly understood. Since Gem has a potential to increase residual DNA damage in cells after radiation and also inhibits the repair pathway in irradiated cells (6), the hypothesis was that Gem may potentiate ^{212}Pb-TCMC (2-(4-isothiocyanatobrenzyl-1,4,7,10-tetraaza-1,4,7,10,tetra-(2-carbamonylmethyl)-cyclododecane)-trastuzumab-induced apoptosis by regulating DNA damage response. A recent study from this laboratory demonstrated that the reduction of cell proliferation by ^{212}Pb-TCMC-trastuzumab is associated with blocked DNA damage repair by interfering with Rad51 (7). The purpose of the experimental design herein was to evaluate the mechanisms of cell death associated with combination treatment, and to allow for a true direct comparison to prior published therapy studies. The *in vivo* studies reported herein were performed by treating mice at 3 days post-tumor inoculation with ^{212}Pb-labeled mAb (trastuzumab). The mice had been pre-treated with Gem 24 h earlier. Tumors were then harvested for analysis. The data described herein demonstrate that the cell killing efficacy of this combination therapy in the LS-174T i.p. xenograft model may be associated with the abrogation of the DNA damage check point, blocked DNA damage repair, and chromatin remodeling, leading to the potentiation of ^{212}Pb-TCMC-trastuzumab-induced apoptosis by gemcitabine.

METHODS AND MATERIALS

Cell line and reagents

The human colon carcinoma cell line (LS-174T) was used for all *in vivo* studies. LS-174T was grown in a supplemented DMEM. All media and supplements were obtained from Lonza (Walkersville, MD). pCdc2^{Y15}, pChk1^{S295}, pChk1^{S345}, pCdc25C^{S216}, pH3^{S10} antibodies were purchased from Cell Signaling (Danvers, MA) and Rad51 antibody was obtained from Abcam (Cambridge, MA).

Chelate synthesis, mAb conjugation, and radiolabeling

The synthesis, characterization, and purification of the bifunctional ligand TCMC have been previously described (8). Trastuzumab (Herceptin®; Genentech, South San Francisco, CA) was conjugated with TCMC by established methods using a 10-fold molar excess of ligand to mAb. A 10 mCi ^{224}Ra/^{212}Pb generator was purchased from AlphaMed (Lakewood, NJ). HuIgG was also conjugated with the TCMC ligand and radiolabeled, providing a non-specific control antibody for the experiments (9).

Tumor model, treatment and tumor harvesting

Studies were performed with 19–21 g female athymic mice (NCI-Frederick) bearing 3 d i.p. LS-174T xenografts (9). The viability of the LS-174T cells (> 95 %) was determined using trypan-blue. Mice were injected i.p. with 1×10^8 LS-174T cells in 1 mL of DMEM. Gemcitabine (Eli Lilly, Indianapolis, IN) was prepared for injection (1 mg in 0.5 mL PBS) and administered by i.p. injection to the mice 2 d after injection of the LS-174T cells. ^{212}Pb-TCMC-trastuzumab (10 μCi in 0.5 mL PBS) was administered to the mice (n = 10–15) 24 h later. Mice utilized for the cell cycle and proliferation studies (n = 5) were injected i.p. with 5-bromo-2′-deoxyuridine (BrdU; 1.5 mg in 0.5 mL PBS; Sigma) 4 h prior to euthanasia.

The i.p. tumors were harvested from mice at 6, 24, 48, 72, 96 and 120 h post injection the labeled antibodies.

Flow cytometry

Cell cycle distribution and DNA synthesis were determined by flow cytometry (10) on a FACSCalibur instrument (BD Biosciences, San Jose, CA). DNA content (propidium iodide) and DNA synthesis (BrdU content) were analyzed using two parameter data collection with CellQuest (BD Biosciences) software while single parameter DNA distribution was performed and analyzed using Modfit LT ver. 3.0 (Verity Software House, Topsham, ME).

Determination of apoptosis

Apoptotic bodies were scored using hematoxylin and eosin (H&E) staining (11). Five fields were analyzed per tumor section, and the number of apoptotic bodies per 100 nuclei scored expressed as a percentage. The presence of apoptotic bodies on tumor sections was also determined using the Dead End Fluorometric TUNEL System (Promega, Madison, WI). Tissue sections were mounted using Vectashield with DAPI (Vector Laboratories, Burlingame, CA) to counterstain DNA. Images were visualized by Olympus FV300 equipped with FluoView software (Center Valley, PA).

Immunohistochemistry

Immunohistochemistry (IHC) was performed as described in the manufacturer's instructions (Cell Signaling, Danvers, MA) with some modifications. After staining, tissue sections were mounted using Cytoseal XYL (Thermo Scientific, Rockford, IL).

Comet assay

Sample preparation was performed according to the tissue preparation protocol in the manufacturer's instructions (Trevigen, Gaithersburg, MD). The neutral comet assay was performed as described in the manufacturer's instructions. Sixty comets per individual preparation were scored and all measurement parameters were calculated on CometScore (TriTek, Sumerduck, VA).

Chromatin immunoprecipitation

The chromatin immunoprecipitation assay (ChIP) was utilized to determine whether histone methylation was altered by [212]Pb-TCMC-trastuzumab therapy. The ChIP assay Kit (Upstate, Billerica, MA) was used according to the manufacturer's instructions with minor adjustments. Immunoprecipitated DNA was analyzed by quantitative real time PCR (qPCR) using p21 promoter specific primers (Primer sequences are available upon request).

Statistics

At least three independent experiments were performed for each data point described. All values were expressed as the mean ± S.D. Student's test was used for paired data, and multiple comparisons were performed with the ANOVA. A p-value < 0.05 was considered statistically significant.

RESULTS

Gemcitabine potentiates [212]Pb-TCMC-trastuzumab-induced apoptosis

Mice bearing a 3 day tumor burden were treated with [212]Pb-TCMC-trastuzumab following a 24 h pre-treatment with Gem as illustrated by the scheme in Figure 1A. To determine whether Gem could potentiate [212]Pb-TCMC-trastuzumab induced apoptosis, IHC techniques

and the TUNEL assay were utilized. At 6 to 24 h after administration of the ^{212}Pb-TCMC-trastuzumab in mice that were pre-treated with Gem (Figure 1B), quantitation of the apoptotic bodies suggests that there was an enhanced tumor cell killing (Gem/^{212}Pb-TCMC-trastuzumab *vs* Gem alone, $p < 0.01$ at 6h & 24h; Gem/^{212}Pb-TCMC-trastuzumab *vs* Gem/^{212}Pb-TCMC-HuIgG, $p < 0.05$ at 6h). A relatively high apoptotic rate was also observed in the non-specifically targeted control, ^{212}Pb-TCMC-HuIgG, at 24 h after injection, compared to no treatment, which was increased in response to Gem, suggesting a general effect of α-particle irradiation in response to Gem that can not be overlooked due to a result of the quantity of ^{212}Pb in the tumor, whether bound to HER2 or not. Results of the TUNEL assay indicate that Gem alone exerted a minimal effect on the induction of apoptosis. In contrast, a higher apoptotic rate was observed with the combination of ^{212}Pb-TCMC-trastuzumab and Gem pre-treatment (Figure 1C).

^{212}Pb-TCMC-trastuzumab in response to gemcitabine induces abrogation of the G2/M arrest

To examine the effect of ^{212}Pb-TCMC-trastuzumab on DNA synthesis and cell cycle distribution in response to Gem, tumor bearing mice were injected (i.p.) with BrdU to pulse-label the tumor xenografts for evaluation of DNA synthesis. Illustrated in Figure 2, there was a noticeable decrease in BrdU incorporation (4.7 % ± 1.4) 24 hours after ^{212}Pb-TCMC-trastuzumab following Gem pre-treatment compared to BrdU uptake by the tumors from untreated mice (23.8 % ± 1.3). A relatively high depression of DNA synthesis was also observed in ^{212}Pb-TCMC- HuIgG in response to Gem, indicating the general effect of α-particle irradiation. Furthermore, the inhibition of cell proliferation in tumors that were treated with Gem alone was not as great as what was observed ($p < 0.01$) in the group that received Gem followed by the ^{212}Pb-TCMC-trastuzumab (Figures 2 and Table S1).

Next, the effect of ^{212}Pb-TCMC-trastuzumab on cell cycle distribution after Gem pre-treatment was analyzed. Cell cycle arrest in the S-phase was evident but there was not a corresponding increase in the S-phase of Gem/^{212}Pb-TCMC-trastuzumab vs. Gem/^{212}Pb-TCMC-HuIgG or Gem alone at 24 h (Figure 3 and Table S2). Following the treatment with ^{212}Pb-TCMC-trastuzumab after Gem pre-treatment, there was a rapid S-phase arrest (40.2% ± 1.0) at 6 h compared to the controls, ^{212}Pb-TCMC-HuIgG with Gem pre-treatment and Gem alone. Notably, there was a marked decrease (4.9%) in the G2/M-phase fraction of the cell cycle (Gem/^{212}Pb-TCMC-trastuzumab *vs* Gem alone or Gem/^{212}Pb-TCMC-HuIgG; p < 0.01 at 6 h) with a corresponding increase in the S-phase at 6 to 24 h, compared to the controls, ^{212}Pb-TCMC-HuIgG with Gem or Gem alone. After 24 h, the elevated G2/M-phase arrests were maintained throughout the study period in mice treated with ^{212}Pb-TCMC-trastuzumab after Gem pre-treatment. In contrast, the cell cycle distribution in the G2/M-phase was lower after 48 h in the mice treated with Gem/ ^{212}Pb-TCMC-HuIgG ($p < 0.05$ at 48, 72, & 96 h, Figure 3 and Table S2).

^{212}Pb-TCMC-trastuzumab inhibits Chk1 phosphorylation after gemcitabine pre-treatment

In the presence of DNA damage, activated Chk1 inactivates the Cdc25C by phosphorylating Cdc25C at Ser216, and in turn prevents the activation of the cyclin B/Cdc2 mitotic kinase complex, resulting in G2 cell cycle arrest and suppression of mitosis (12, 13). To assess the effect of ^{212}Pb-TCMC-trastuzumab on Chk1 activation in S-phase arrested tumors induced by Gem, the ATR/Chk1 signaling pathway was examined. Analysis of Chk1 phosphorylation demonstrated that in the tumor samples from mice that were treated with Gem alone or ^{212}Pb-TCMC-HuIgG with Gem pre-treatment, there was a marked increase in Chk1 phosphorylation. In contrast, ^{212}Pb-TCMC-trastuzumab treatment in response to Gem inhibited phosphorylation of Chk1 at 6 to 24 h (Figure 4A). The ability of Chk1 to undergo autophosphorylation was also inhibited in the tumors from mice treated with the

combination of Gem and ^{212}Pb-TCMC-trastuzumab (Figure 4B). The cytoplasmic staining of phosphorylated Cdc25C of the tumors from the group that were administered ^{212}Pb-TCMC-trastuzumab pretreated with Gem was suppressed. ^{212}Pb-TCMC-trastuzumab administration post Gem pre-treatment decreased the phosphorylation of Cdc2 (Figure 4B), suggesting a more pronounced activation of Cdc2. As anticipated, premature mitotic entry, evidenced by induction of phosphorylation of histone H3 at Ser 10, was observed in mice treated with the combination of Gem and ^{212}Pb-TCMC-trastuzumab as compared to the controls (Figure 4A).

After gemcitabine pre-treatment, ^{212}Pb-TCMC-trastuzumab interferes with DNA repair

The findings detailed above suggest that Gem may potentially sensitize the targeted tumor to the cytotoxic effects of ^{212}Pb-TCMC-trastuzumab. To determine the degree of DNA damage affected by ^{212}Pb-TCMC-trastuzumab after Gem pre-treatment, IHC was performed using $\gamma H_2 AX$. The presence of DNA double strand breaks was also evaluated by the neutral comet assay. An intense increase in $\gamma H_2 AX$ phosphorylation was evident by ^{212}Pb-TCMC-trastuzumab after Gem pre-treatment compared to ^{212}Pb-TCMC-HuIgG post Gem pre-treatment or Gem treatment alone (Figure 5A). The neutral comet assay revealed that all treatments resulted in the accumulation of DNA damage compared to the untreated controls as expected. High accumulation of DNA damage occurred early by 6 h post irradiation. The ^{212}Pb-TCMC-trastuzumab treatment following Gem pre-treatment resulted in the greatest increase of DNA damage at 6 compared to all treatment groups that was also significant compared to the non specific control Gem/^{212}Pb-TCMC-HuIgG (Gem/^{212}Pb-TCMC-trastuzumab *vs* Gem/^{212}Pb-TCMC-HuIgG, $p < 0.01$ at 6h). The high induced DNA damage occurred throughout the study period (Gem/^{212}Pb-TCMC-trastuzumab *vs* Gem alone, $p < 0.01$ at 6–24 & 96h, $p < 0.05$ at 48–72 h; Gem/^{212}Pb-TCMC-trastuzumab *vs* Gem/^{212}Pb-TCMC-HuIgG, $p < 0.01$ at 6h, $p < 0.05$ at 48h), suggesting inhibition of the DNA damage repair system that was highest and early in the group that received Gem/^{212}Pb-TCMC-trastuzumab (Figure 5B).

One potential mechanism underlying such observation is that ^{212}Pb-TCMC-trastuzumab can induce blockade of DNA double strand break homologous recombination repair (HRR), in part, due to the down-regulation of Rad51 (14, 15). Therefore, the expression level of Rad51 in each treatment group was assessed by Western blot analysis. The loss of Rad51 following the ^{212}Pb-TCMC-trastuzumab treatment post Gem pre-treatment was most evident at 24 h indicating the accumulation of unrepaired DNA damage (Figure 5C).

^{212}Pb-TCMC-trastuzumab induces modification in chromatin structure of p21 after gemcitabine pre-treatment

Chromatin remodeling is significantly altered in tumors. In order to identify particular changes in the epigenetic marks for open and closed chromatin status in the promoter of *p21*, one of the DNA damage response genes, the histone modifications associated with transcriptionally active chromatin states, such as H3 methylated at lysine 4 and transcriptionally repressed chromatin states, such as H3 methylated at lysine 9, were investigated. The ratio between H3K4 and H3K9 methylations was used as a measurement of changes (open/close) in chromatin structure. Illustrated in Figure 6, histone modifications associated with transcriptionally repressed chromatin states prevailed following the treatment of tumor bearing mice with Gem 24 h before injection of ^{212}Pb-TCMC-trastuzumab, indicating that the combined treatment of Gem and ^{212}Pb-TCMC-trastuzumab induced the delayed open chromatin structure until 72–96 h ($p < 0.001$).

DISCUSSION

Chemotherapy and radiotherapy induce DNA damage. Cells respond by activating genes involved in cell cycle arrest, DNA repair and apoptosis. Gemcitabine has been reported to potentiate the therapeutic efficacy of ^{212}Pb-TCMC-trastuzumab (16). The high LET of α-particle radiation has been proposed as ideal for the treatment of smaller tumor burdens, micrometastatic disease, and peritoneal disease. In this study, the evidence supporting molecular mechanisms on the sensitization of tumors to ^{212}Pb-TCMC-trastuzumab treatment by Gem pre-treatment was investigated in the LS-174T i.p. xenograft model.

One potential consequence of an increase in residual DNA damage after radiation in Gem treated cells is an increase in radiation-induced apoptosis (17). The effect of ^{212}Pb-TCMC-trastuzumab treatment following Gem pre-treatment on the level of apoptosis was evident compared to the controls at earlier time points, suggesting that ^{212}Pb-TCMC-trastuzumab treatment in response to Gem may be associated with the potentiation of cell killing efficacy in this i.p. colon cancer xenograft model. Gemcitabine is known to affect a block in the early S-phase of the cell cycle which has been correlated with the radiosensitization of tumor cells (18). According to current understanding, the kinases ATR and Chk1 play critical roles in this checkpoint. Gemcitabine treatment of the LS-174T i.p. tumor xenografts followed by ^{212}Pb-TCMC-trastuzumab resulted in an early increase of S-phase. Notably, there was a decrease of G2-M arrest at the earlier time points (6 to 24 hours), likely attributable to the inhibition of Chk1 phosphorylation by this combined treatment, suggesting that inhibition of Chk1 phosphorylation in the ATR/Chk1 signaling pathway may be correlated with the induction of apoptosis. This result is in agreement with prior observations that the G2-phase abrogation prevents cancer cells from repairing DNA damage at early stages of replication leading to apoptotic cell death (19). Therefore, it appears that the inhibition of Chk1 phosphorylation with corresponding abrogation of G2/M-phase cell cycle arrest is required for maximal sensitization of tumors from mice treated with ^{212}Pb-TCMC-trastuzumab post Gem pre-treatment, resulting in apoptosis at earlier time points.

HRR is preferentially used in the late S and G2 phases of the cell cycle (20). ^{212}Pb-TCMC-trastuzumab administered after Gem pre-treatment led to a marked increase in DNA damage at earlier time points (6–24 hr). The Gem pre-treatment of tumors treated with ^{212}Pb-TCMC-trastuzumab resulted in down-regulation of Rad51 expression, suggesting that the increase in DNA damage and the inhibition of DNA damage repair may be associated with the maximal sensitization, resulting in apoptosis at earlier time points. In addition, epigenetic markers for open/closed chromatin status using the H3K4/H3K9 ratio revealed that modifications in the chromatin structure of *p21* may be associated with transcriptionally repressed chromatin states such as H3 methylation at lysine 9 at earlier time points. This would indicate a failure of adequate *p21* induction at earlier time points due to the delay in open chromatin structure of *p21* that correlated to active transcription induced by ^{212}Pb-TCMC-trastuzumab after Gem pre-treatment.

In summary, there appears to be a strong correlation between the inhibition of Chk1 phosphorylation, interference with HRR through the down-regulation of Rad51, and chromatin modification at earlier time points. These data suggest that the cell cycle perturbation followed by the induction of apoptosis plays an important role in the sensitization effect observed by the combination of ^{212}Pb-TCMC-trastuzumab preceded by Gem. Thus, these mechanistic studies could provide additional insights for new strategies for the design of clinical trials that combine α-radioimmunotherapy and chemotherapeutics.

Supplementary Material

Refer to Web version on PubMed Central for supplementary material.

Acknowledgments

References

1. Ries, LAG.; Melbert, D.; Krapcho, M., et al. SEER Cancer Statistics Review, 1975–2005. Bethesda (MD): National Cancer institute; 2008.

2. Toschi L, Finocchoaro G, Bartolini S, et al. Role of gemcitabine in cancer therapy. Future Oncol. 2005; 1:7–17. [PubMed: 16555971]

3. Yong K, Brechbiel MW. Towards translation of ^{212}Pb as a clinical therapeutic; getting the lead in! Dalton Trans. 2011; 40:6068–76. [PubMed: 21380408]

4. Friesen C, Glatting G, Koop B, et al. Breaking chemoresistance and radioresistance with ^{213}Bi anti-CD45 antibodies in leukemia cells. Cancer Res. 2007; 67:1950–58. [PubMed: 17332322]

5. Suoio S, Gouard S, Charrier J, et al. Mechanisms of cell sensitization to α-radioimmunotherapy by doxorubicin or paclitaxel in multiple myeloma cell lines. Clin Cancer Res. 2005; 11:7047–52.

6. Wachters FM, van Putten JW, Maring JG, et al. Selective targeting of homologous DNA recombination repair by gemcitabine. Int J Radiat Oncol Biol Phys. 2003; 57:553–62. [PubMed: 12957269]

7. Yong KJ, Milenic DE, Baidoo KE, et al. ^{212}Pb-Radioimmunotherapy induces G2 cell cycle arrest and delays DNA damage repair in tumor xenografts in a model for disseminated intraperitoneal disease. Mol Cancer Ther. 2012; 11:639–48. [PubMed: 22238365]

8. Chappell LL, Dadachova E, Milenic DE, et al. Synthesis, characterization, and evaluation of a novel bifunctional chelating agent for the lead isotopes ^{203}Pb and ^{212}Pb. Nucl Med Biol. 2000; 27:93–100. [PubMed: 10755652]

9. Milenic DE, Garmestani K, Brady ED, et al. α-particle radioimmunotherapy of disseminated peritoneal disease using a ^{212}Pb-labeled radioimmunoconjugate targeting HER2. Cancer Biother Radiopharm. 2005; 20:557–68. [PubMed: 16248771]

10. Grégoire V, Van NT, Stephens LC, et al. The role of fludarabine-induced apoptosis and cell cycle synchronization in enhanced murine tumor radiation response *in vivo*. Cancer Res. 1994; 54:6201–09. [PubMed: 7954467]

11. Stephens LC, Ang KK, Schultheiss TE, et al. Apoptosis in irradiated murine tumors. Radiat Res. 1991; 127:308–16. [PubMed: 1886987]

12. Sanchez Y, Wong C, Thomas RS, et al. Conversation of the Chk1 checkpoint pathway in mammals: linkage of DNA damage of Cdk regulation through CDC25. Science. 1997; 277:1497–01. [PubMed: 9278511]

13. Liu Q, Guntuku S, Cui XS, et al. Chk1 is an essential kinase that is regulated by ATR and required for G2/M DNA damage checkpoint. Gene Dev. 2000; 14:1448–59. [PubMed: 10859164]

14. Dai Y, Grant S. New insights into checkpoint kinase 1 in the DNA damage response signaling network. Clin Cancer Res. 2010; 16:376–83. [PubMed: 20068082]

15. Bahassi EM, Ovesen JL, Riesenberg AL, et al. The checkpoint kinase Chk1 and Chk2 regulate the functional associations between hBRCA2 and Rad51 in response to DNA damage. Oncogene. 2008; 27:3977–85. [PubMed: 18317453]

16. Milenic D, Garmestani K, Brady ED, et al. Potentiation of high-LET radiation by gemcitabine: targeting HER2 with Trastuzumab to treat disseminated peritoneal disease. Clin Cancer Res. 2007; 13:1926–35. [PubMed: 17363549]

17. Lawrence TS, Blackstock AW, McGinn C. The mechanism of action radiosensitization of conventional chemotherapeutic agents. Semin Radiat Oncol. 2003; 13:13–21. [PubMed: 12520460]

18. Morgan MA, Parsels LA, Zhao L, et al. Mechanism of radiosensitization by the Chk1/2 inhibitor AZD7762 involves abrogation of the G2 checkpoint and inhibition of homologous recombinational DNA repair. Cancer Res. 2010; 70:4972–81. [PubMed: 20501833]

19. Bucher N, Britten C. G2 checkpoint abrogation and checkpoint kinase-I targeting in the treatment of cancer. Br J Cancer. 2008; 98:523–528. [PubMed: 18231106]

20. Wachers FM, van Putten JWG, Maring JG, et al. Selective targeting of homologous DNA recombination repair by gemcitabine. Int J Radiat Oncol Biol Phys. 2003; 58:353–360.

SUMMARY

The mechanism(s) of cell death induced by the targeted delivery of high LET radiation remains unresolved. We demonstrate that the cell killing efficacy of [212]Pb-TCMC-trastuzumab following gemcitabine pre-treatment may be associated with abrogation of the G2/M checkpoint, inhibition of DNA damage repair, and chromatin remodeling, resulting in the potentiation of [212]Pb-TCMC-trastuzumab-induced apoptosis by Gem in the LS-174T i.p. xenograft model.
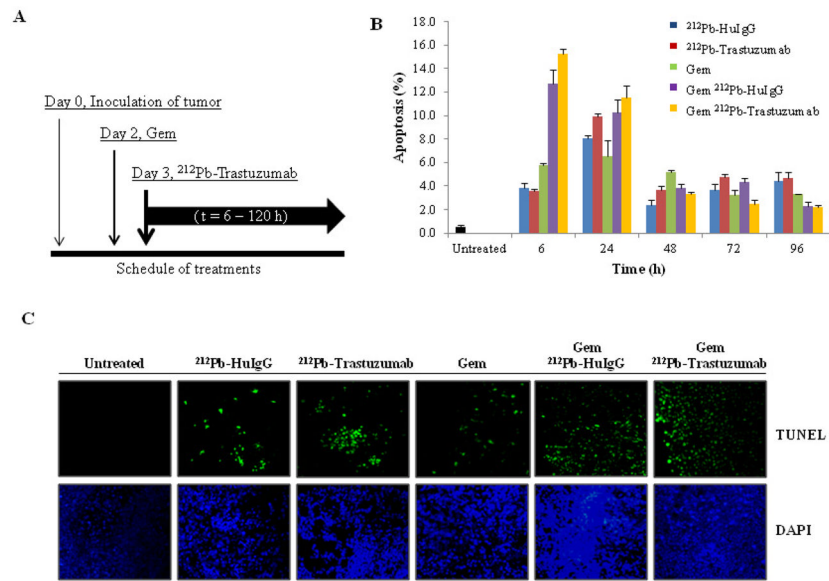
Figure 1. Induction of apoptosis in LS-174T xenografts model

A. Treatment Schedule. Mice bearing i.p. LS-174T xenografts were treated with Gem followed by ^{212}Pb-TCMC-trastuzumab at the indicated time points. Additional groups included untreated, Gem alone, ^{212}Pb-TCMC-trastuzumab, and ^{212}Pb-TCMC-HuIgG with/ without Gem pre-treatment.

B. Apoptosis induced by ^{212}Pb-TCMC-trastuzumab in response to Gem. The apoptotic nuclei at the indicated time points were counted under light microscopy; 500 nuclei were scored per tumor. Results represent the average of a minimum of three replications ($\pm$ SD).

C. Fluorescence microscopy images of apoptosis at 24 h. Paraffin-embedded sections at 24 h were stained with TUNEL. Top, TUNEL staining; bottom, DAPI counter staining (40x)
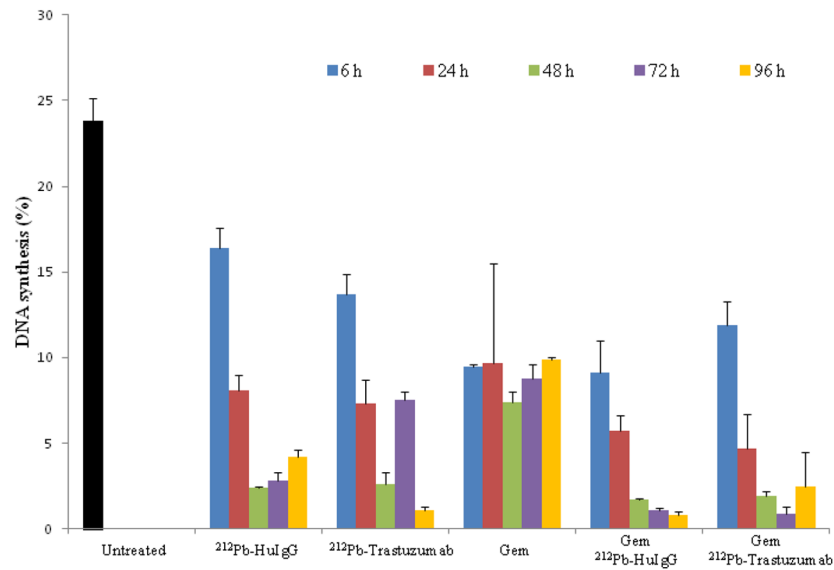
Figure 2. Analysis of DNA synthesis
Mice (n=5) bearing i.p. LS-174T xenografts were treated with ^{212}Pb-TCMC-trastuzumab with Gem pre-treatment at the indicated time points. In the same day, mice bearing i.p. tumor xenografts were injected with BrdU 4 hours prior to tumor collection to evaluate DNA synthesis.
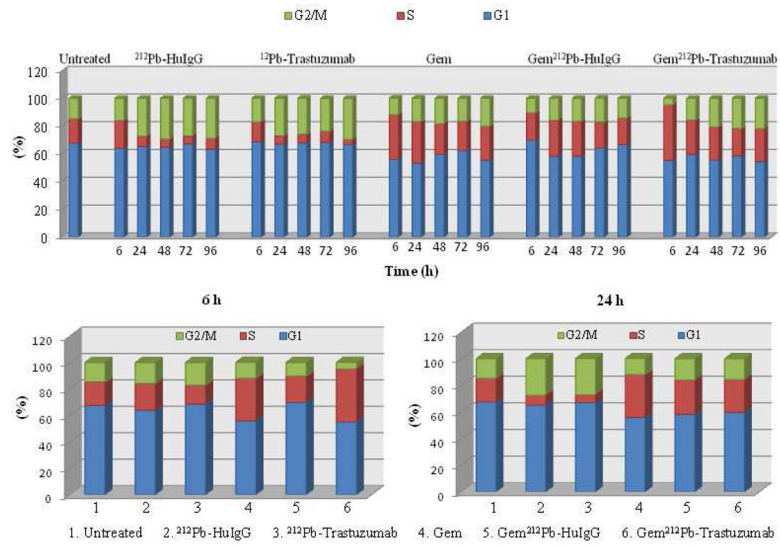
Figure 3. Analysis of cell cycle distribution
Mice bearing i.p. tumor xenografts were injected with BrdU 4 hours prior to tumor collection to pulse-label the tumor xenografts to evaluate cell cycle distribution. The nuclei were isolated, stained with propidium iodide, and the DNA analyzed for cell cycle distribution. Results at the indicated time points represent the average of a minimum of three replicates (±SD).
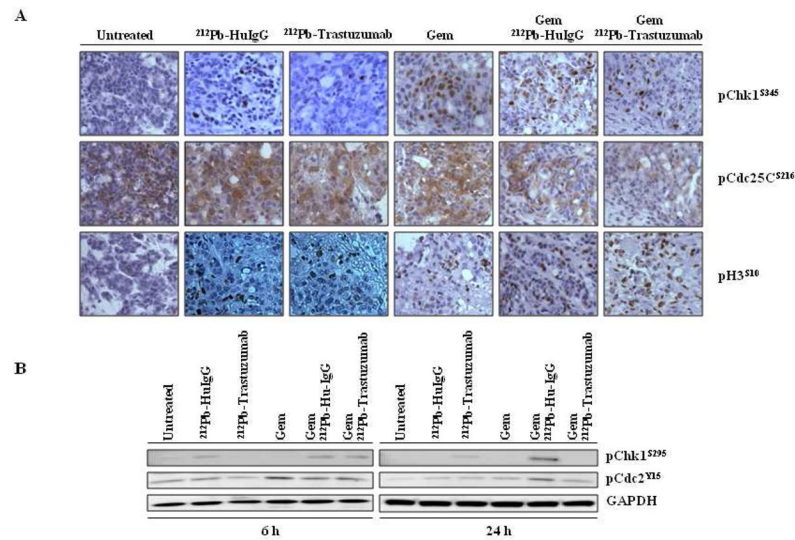
Figure 4. Inhibition of Chk1 induced by ^{212}Pb-TCMC-trastuzumab with Gem pre-treatment
A. Light microscopy images of paraffin-embedded sections. Sections were stained with antibodies of pChk1at S345 and pCDC25C at S216, and pH3 at S10. The sections from the 24 h time point are shown. Representative images of three individual specimens are shown. Top: pChk1, middle: pCDC25C, bottom: pH3
B. Western blotting images. Immunoblot analysis for pChk1 at Ser295 and pCdc2 at Tyr15 was performed at the indicated time points. The pChk1 (S295) detected was 56 kDa and the pCdc2 (Tyr15) detected was 34 kDa. The equivalent protein loading control was GAPDH.
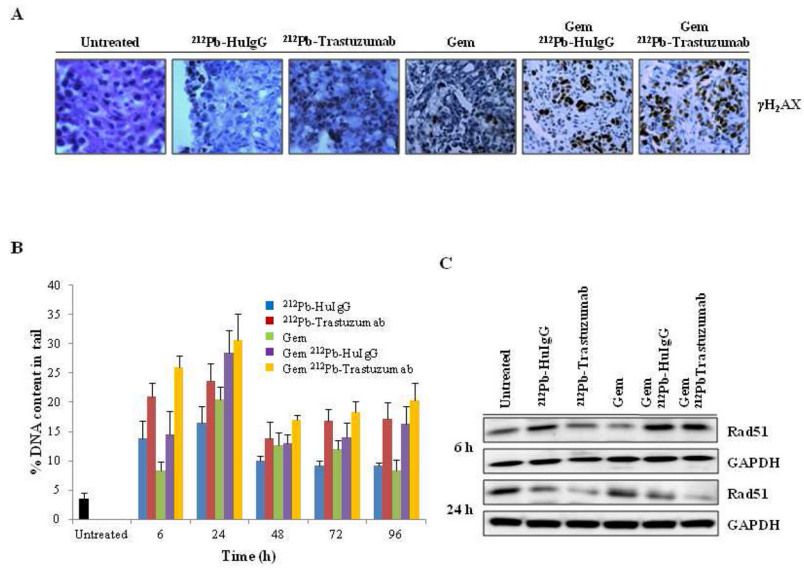
Figure 5. Effect of ^{212}Pb-TCMC-trastuzumab with Gem pre-treatment on DNA damage repair
A. Light microscopy microscopy images of IHC at 24 h. Sections were stained with antibody of γH$_2$AX at 24 h. The sections from the 24 h time point are shown.
B. DNA contents in tail moment measured by comet assay. DNA damage was quantified by DNA contents in tail at the indicated times. Results represent the average of minimum of three replications (± SD).
C. Down-regulation of Rad51 expression. Immunoblot analysis for Rad51 was performed at the indicated time points. Rad51 detected was 37 kDa. The equivalent protein loading control was GAPDH.
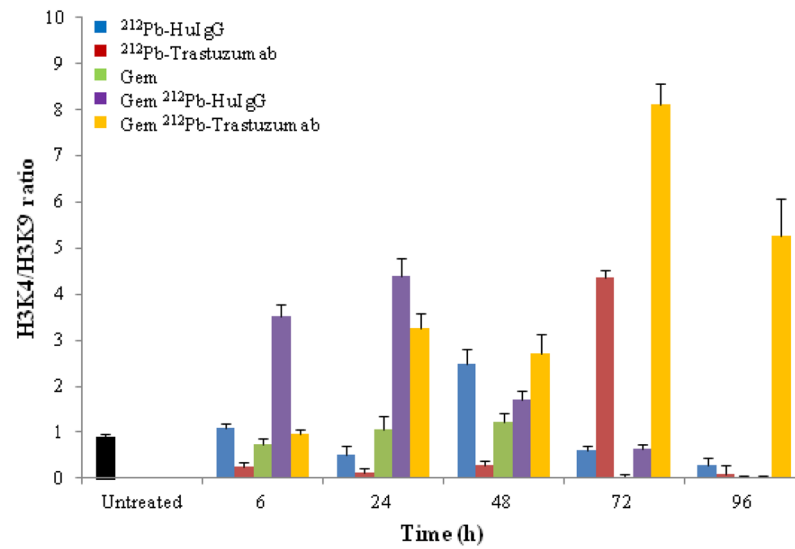
Figure 6.
Effect of [212]Pb-TCMC-trastuzumab with Gem pre-treatment on chromatin remodeling. ChIP assay was performed using *p21* promoter specific primer at the indicated time points and quantified using a real time quantitative PCR. Results represent the average of minimum of three replications (± SD).